Available online at www.joac.info

ISSN: 2278-1862

Journal of Applicable Chemistry, 2012, 1 (2):272-287

(International Peer Reviewed Journal)

Symmetric Supercapacitors Employing MnO_2 And Polyaniline Composite

C. Selvaraj[1], Surender Kumar [1], A. R. Raju [2] and N. Munichandraiah [1*]

1. Department of Inorganic and Physical Chemistry, Indian Institute of Science, Bangalore-560012, India
2. Honeywell Technology Solutions Labs Pvt. Ltd., Bannerghatta Road, Bangalore - 560226, India

E-mail: muni@ipc.iisc.ernet.in

ABSTRACT

Large area electrodes of MnO_2 + polyaniline (PANI) composites of several compositions are fabricated with high specific mass of the active materials. Laboratory scale symmetric capacitors consisting of two similar electrodes separated by absorbent glass mat soaked in aqueous $Mg(NO_3)_2$ electrolytes are assembled. The capacitor made with a composite of MnO_2+5 wt% PANI provides high capacitance and low equivalent series resistance. The results of long-cycle life test conducted for the capacitors suggest that the capacitance of MnO_2+5 wt% PANI capacitor is stable over 1000 charge-discharge cycles and the capacitance is greater than that of MnO_2 capacitor. Ac impedance data suggest that the charge-transfer resistance (R_{ct}) associated with Mn^{4+}/Mn^{3+} redox process, which is noticeable at high frequency region is associated with build-up of pseudocapacitance, which is noticed at low frequency region. There is a gradual increase in R_{ct} during the initial stages of cycling and thereafter it remains unchanged. MnO_2+5 wt% PANI composite is found to be suitable for development of commercial capacitors.

Keywords: Manganese dioxide, Polyaniline, Composites, Supercapacitors, Ac impedance.

INTRODUCTION

There has been an increasing interest on research and development of electrochemical supercapacitors in recent years[1, 2]. Among several materials investigated as the active

materials of supercapacitors, MnO_2 is very attractive as it is non-toxic, environmental-friendly, easy to synthesize, stable at ambient environments, and also it has abundant natural resources. Furthermore, MnO_2 is a well studied material in the area of batteries for several years[3]. MnO_2 exists in several crystallographic forms, which include α, β, γ, δ and λ structures[4]. These structures differ from each other in the way how MnO_6 octahedra are interlinked in the unit cell [3]. It is known that γ-MnO_2 is suitable for battery application and electrolytic MnO_2 (generally known as EMD) used for primary batteries has the γ-structure[5, 6]. On the other hand, it is reported that α- and δ- forms of MnO_2 are suitable for electrochemical supercapacitor application [7, 8]. The reason for applicability of different structures for battery and supercapacitor studies could be attributed to the occurrence of Mn^{4+}/Mn^{3+} redox reaction on surface of MnO_2 particles or films in the case of supercapacitors, whereas the reaction is a bulk process in the case of batteries.

Starting with the report by Lee and Goodenough in 1992[9] on capacitance behaviour of MnO_2 in neutral electrolytes, several reports have appeared[10-15]. The specific capacitance of MnO_2 is in range 150-200 F g^{-1}, which is normally measured on the basis of single electrode studies. Taking account of reversible conversion of Mn^{4+}/Mn^{3+} available in MnO_2 excluding water and other ions adsorbed, absorbed or intercalated, a theoretical specific capacitance of about 1110 F g^{-1} is expected over a potential window of 1.0 V. Although attempts are made to enhance specific capacitance by using nano-structured MnO_2 and composite materials, the gap between the theoretical specific capacitance and practical values remains large. This is due to the fact that pseudocapacitive redox reaction is limited to the surface region of MnO_2 particles or films, and the bulk particle is not utilized for this purpose. Furthermore, the electronic conductivity of MnO_2 is low ($1x10^{-5}$ - $1x10^{-6}$ S cm^{-1})[16], and conducting carbons are generally mixed with MnO_2 for preparation of electrodes. It was found that nearly 30 wt% of acetylene black was required for observing capacitance behaviour of MnO_2[17].

A few conducting polymers have been investigated as additives to MnO_2 for improving its capacitance properties. Among the generally known conducting polymers, polyaniline (PANI) is more interesting than the rest as it is easy to synthesize, inexpensive and environmentally stable. A composite of MnO_2 and PANI was prepared by a redox reaction between $KMnO_4$ and aniline and investigated for capacitance properties[18]. Values of SC in the range of 250-500 F g^{-1} in 0.1 M Na_2SO_4 electrolyte were reported by cyclic voltammetry[18]. In another study, MnO_2-PANI composite was prepared in an organic medium and SC of about 330 F g^{-1} was obtained from galvanostatic charge-discharge cycling studies[19]. Hybrid films of MnO_2-PANI were electrochemically deposited on a carbon cloth from an electrolyte consisting of $MnSO_4$ and aniline [20]. The electrochemical activity in 1M $NaNO_3$ was examined by cyclic voltammetry and charge-discharge cycling. Specific capacitance of about 530 F g^{-1} at a current density of 2.4 mA cm^{-2} was reported[20]. Specific capacitance values reported are 384 F g^{-1} for MnO_2-carbon nanotube modified by PANI[21], 1290 F g^{-1} for electrochemically deposited MnO_2-PANI on stainless steel in an organic electrolyte[22], 510 F g^{-1} for MnO_2-PANI nano composite prepared by insitu polymerization reaction[23], 330 F g^{-1} for MnO_2-PANI composite modified by a silane coupling reagent[24] and 330 F g^{-1} for MnO_2-PANI and multiwall carbon nanotube composite [25]. Differences in the reported values of SC are due to differences in experimental conditions, such as loading levels of the active materials, current densities employed, potential window, etc.

In the above studies, small electrodes (typical area: 1 cm^2) were employed at low loading levels (1-3 mg cm^{-2}) and the results were reported based on measurements employing single electrodes. However, practical applications demand large area electrodes with high loading levels of active

materials. Furthermore, results of a symmetrical capacitor consisting of two identical electrodes throw light directly on the properties of a device. In the present study, large area (9 cm^2) electrodes of MnO_2, and composites of MnO_2 and PANI with high loading level (about 18-20 mg cm^{-2}) are fabricated, laboratory scale symmetric two-electrode capacitors are assembled and characterized by various electrochemical techniques. Among several compositions of MnO_2 + PANI composites studied, supercapacitors fabricated with MnO_2 + 5 wt% PANI provides a high capacity and a low equivalent series resistance.

MATERIALS AND METHODS

All analytical grade chemicals were used for experiments. Potassium permanganate (S D Fine Chem Ltd), ammonium persulphate (Ranbaxy), ethylene glycol (Sisco), aniline (Merck), HNO_3 (NICE Chemicals), H_2SO_4 (S D Fine Chem Ltd), Ketjen black(AKZO Noble Polymer Chem Ltd), PTFE suspension (Aldrich) and magnesium nitrate (S D Fine Chem Ltd) were used as received. All solutions were prepared using doubly distilled water. Commercial grade (304) stainless steel gauge (60 mesh, woven, 0.53 mm diameter wire) was used as the current collector. The stainless steel gauge was sectioned into 3 cm x 3 cm square shaped current collectors with tags at one of the edges. The flag-type current collector was etched in 5 M HNO_3 for 2 min, cleaned thoroughly with doubly distilled water, rinsed with acetone, air-dried and weighed. MnO_2 was prepared from $KMnO_4$ by reduction using ethylene glycol as a reducing agent, as reported previously [26]. In a typical synthesis, 3.16 g $KMnO_4$ was dissolved in 200 ml doubly distilled water. Then 5 ml ethylene glycol was added drop-wise while stirring the solution constantly with a magnetic paddle. Stirring was continued till completion of the reaction, which lasted about 6 h. The brown precipitate was filtered, washed twice with doubly distilled water and finally with ethanol. The product was dried in an oven at 60° C for about 6 h. For preparation of polyaniline, 5 ml aniline was dissolved in 100 ml 1 M H_2SO_4. Then, 5 wt% of ammonium persulphate solution was added drop-wise while the aniline containing beaker was cooled in an ice bath. The product, PANI was repeatedly washed by 1M H_2SO_4. For fabrication of a MnO_2 + 5 wt% PANI composite electrode, MnO_2, Ketjen black carbon, PANI, and PTFE (as suspension) were taken in a weight ratio 60:30:5:5 and thoroughly ground in a mortar. Then resulting dough was rolled into a sheet on a glass plate. The sheet of electrode material was placed on pre-treated SS current collector and compacted under 5 ton pressure. The electrode was dried in an oven at 60^0 C for 6 h. Using this procedure; electrodes were made with 0, 5, 10 and 20 wt% PANI. For fabrication of a capacitor, two electrodes of identical composition were used. Glass absorbing mat (AGM) was employed as a separator. A 3 cm x 3 cm size piece of AGM was soaked in a saturated solution of $Mg(NO_3)_2$, excess solution was drained off and placed in between the two electrodes. The sandwich was enclosed between two thin sheets of perspex and an insulation tape was pasted around to obtain a capacitor. The stainless steel mesh tags were used to take electrical contacts. Scanning electron micrographs of the electrodes were recorded using a microscope model SIRION. Cyclic voltammetry and charge – discharge cycling of the capacitors were carried out by using a CH Instruments potentiostat /galvanostat model 440. Electrochemical impedance spectra were recorded by using EG&G PARC electrochemical impedance analyzer model 6310. The excitation signal was 5 mV (rms) at open-circuit voltage (~ 0 V) of the capacitor. The frequency range was from 100 kHz to 10 mHz. All measurements were carried out in an air-conditioned room at 22±1° C.

RESULTS AND DISCUSSION

Fabrication of capacitors: The particle size of MnO_2 measured by microscopy studies was 5-13 nm and the crystallographic study suggested a poorly crystalline phase of layered δ-structure [26]. The electrochemistry of PANI has been studied and reported widely [27]. It undergoes several redox transformations in acidic electrolytes. PANI alone has been studied for its electrochemical supercapacitor properties in acidic electrolytes [28]. When studying the supercapacitor properties of MnO_2-PANI composites, the electrolyte normally reported in the literature and also in the present work is a neutral salt solution. As the stability of MnO_2 is poor and also it does not exhibit capacitor behavior in acidic electrolyte, neutral electrolytes only are employed. On the other hand, the conductivity of PANI is higher in acidic electrolytes than in neutral electrolytes. Although, the advantages from PANI cannot be fully realized by using it in neutral electrolytes, it is found that the supercapacitor properties of MnO_2-PANI composite in neutral $Mg(NO_3)_2$ electrolyte are superior to the properties of MnO_2 as detailed below. Recent reports suggest that specific capacitance for MnO_2 is greater in electrolyte consisting of Mg^{2+} and Ca^{2+} ions than the conventional Na^+-ion electrolyte [29, 30]. Furthermore, $Mg(NO_3)_2$ is hygroscopic, the electrolyte made out of this salt does not dryout under ambient conditions. This aspect is important in the present experimental conditions because the capacitors were assembled with starved electrolyte conditions in un-sealed containers. It was noticed that capacitors consisting of $NaNO_3$ electrolyte were dried out on storing for a few days and those consisting of $Mg(NO_3)_2$ electrolytes remained wet for several days of storage. SEM micrographs of the as fabricated MnO_2 and MnO_2 + 5 wt% PANI electrodes are shown in Figs. 1a and 1c, respectively. It is seen that the electrode materials are homogenously mixed and the electrodes are compacted uniformly. The particles of individual constituents are not distinguishable.

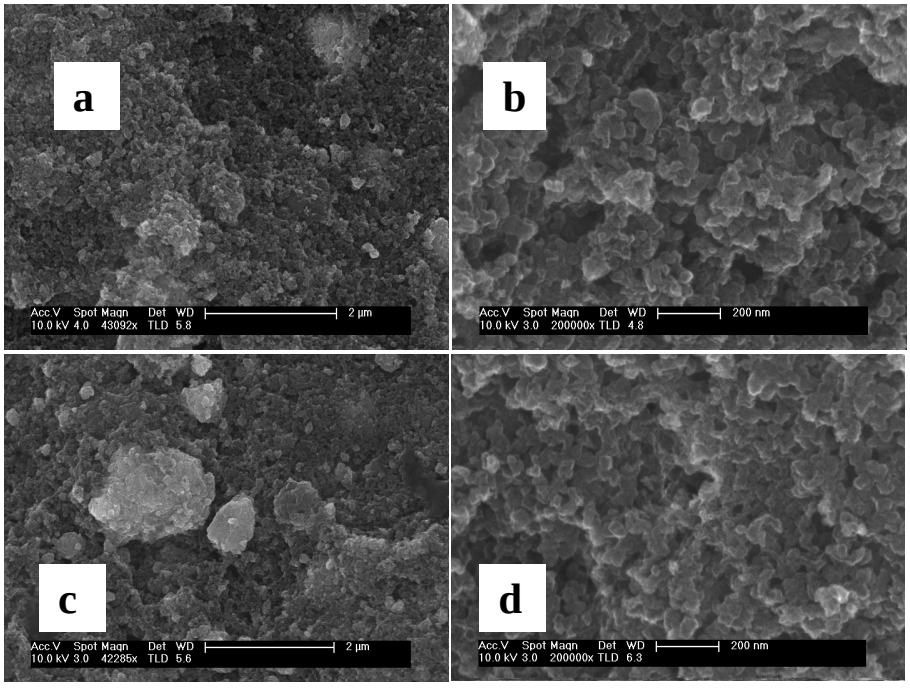

Fig.1 SEM micrographs of (a and b) MnO_2 electrode and (c and d) MnO_2 + 5 wt% PANI before (a and c) and after (b and d) subjecting to 1000 charge-discharge cycles at a current of 100 mA.

Cyclic voltammetry and charge-discharge cycling : Cyclic voltammograms of capacitors made of MnO_2 and MnO_2 + 5 wt% PANI composite are shown in Fig. 2.

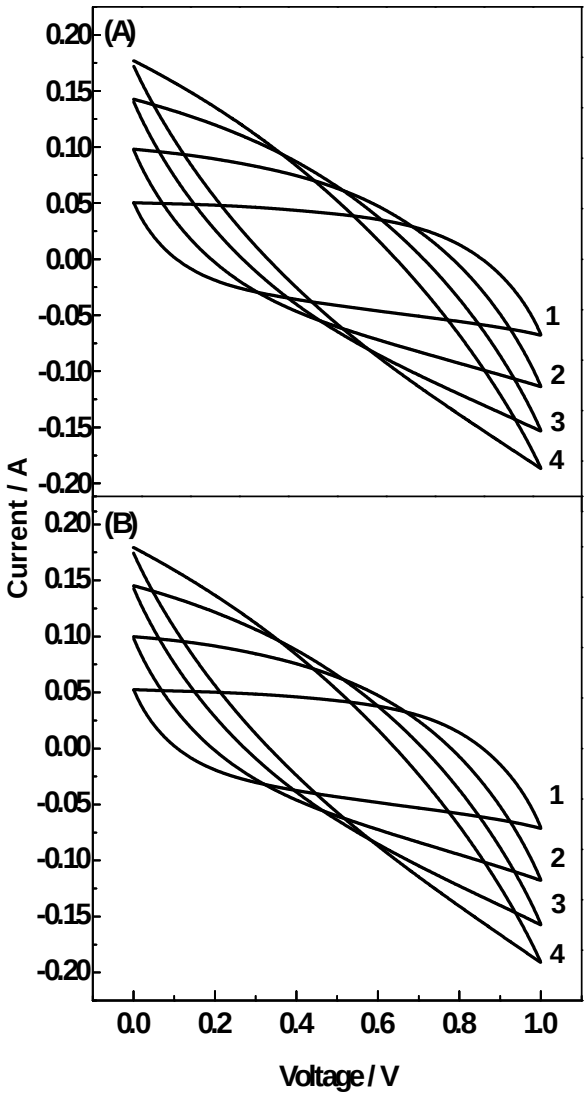

Fig. 2 Cyclic voltammograms of capacitors made of (A) MnO_2 and (B) MnO_2 + 5 Wt% PANI at a scan rate of 2 (1), 5 (2), 10 (3), 20 mV s^{-1} (4).

Similar voltammograms were recorded for other compositions of the composite. At low scan rates the voltammograms look rectangular in shape, but they appear as resistive–capacitive current–voltage curves at high sweep rates. This is attributed to poor electronic conductivity of MnO_2. The effect of PANI present in the composite is not reflected in the voltammograms.
Typical charge-discharge curves of capacitors of different compositions are presented in Fig. 3 at a current of 50 mA.

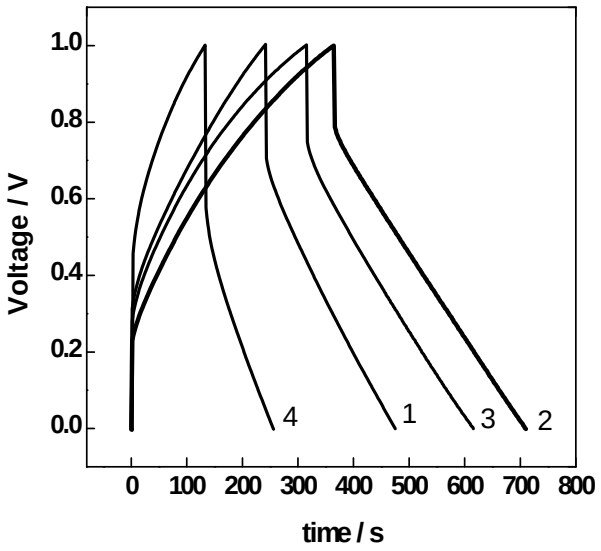

Fig. 3 Charge-discharge curves of MnO_2 capacitors with 0 (1), 5 (2), 10 (3) and 20 wt% (4) PANI at a charge-discharge current of 50 mA.

During charging, there is a sudden rise in voltage from 0 V followed by a linear increase with time up to 1.0 V. Also, there is a sharp decrease in voltage at the commencement of discharge, followed by a linear decrease with time of discharge. The sharp increase or decrease in voltage at the beginning of charge or discharge is attributed to the effect of internal resistance of the capacitors. Linear variation of voltage during charge or discharge is the property of a capacitor, whereas the charge/discharge curve with plateaus is the property of a battery [1]. The charge storage mechanism in MnO_2 capacitor is a surface processes which involves Mn^{4+}/Mn^{3+} redox reaction in solid state. When the surface sites of Mn^{4+} are reduced to Mn^{3+}, there is a simultaneous insertion of cations from the electrolyte on the surface of MnO_2 particles. Considering $Mg(NO_3)_2$ as the electrolyte, the reaction is written as.

$$2\ MnO_2 + Mg^{2+} + 2e^- \rightleftharpoons (MnOO)_2Mg \qquad (1)$$

At the negative electrode the conversion of MnO_2 to $(MnOO)_2Mg$ takes place when the voltage decreases from 1.0 V to 0 V, whereas the conversion of $(MnOO)_2Mg$ to MnO_2 occurs at the positive electrode. At the respective electrodes, the opposite reactions take place when the capacitor voltage increases from 0 to 1.0 V. The total discharge capacitance (C_T) was calculated using eq. (2).

$$C_T = I\ t\ /\ V \qquad (2)$$

where I is discharge current, t is discharge time and V is voltage window (= 1.0 V). From the data presented in Fig. 3, the values of discharge capacitance obtained for MnO_2+PANI composite capacitors with 0, 5, 10 and 20 wt% PANI are 11.6, 17.2, 14.9 and 6.1 F, respectively, and the corresponding values of coulombic efficiency are 97, 95, 96, and 93 % at a discharge current of 50 mA. The discharge current (50 mA) corresponds to a current density of 5.6 mA cm^{-2} (on the basis of electrode geometric area). The specific current values are 0.14, 0.15, 0.16 and

0.21 A g^{-1} (on basis of MnO_2 mass), and 0.14, 0.14, 0.13 and 0.15 A g^{-1} (on the basis of combined masses of MnO_2 and PANI) for capacitor with 0, 5, 10 and 20 wt% PANI, respectively. Taking account of the mass of MnO_2 in the composite on both electrodes of a capacitor, the respective specific capacitance (SC) values of capacitor obtained are 32.8, 51.0, 47.2, and 26.1 F g^{-1}. On the other hand, the respective SC values become 32.8, 47.0, 24.5, and 9.6 F g^{-1} on the basis of combined masses of both MnO_2 and PANI in the composite of both electrodes. In either case, the maximum value of SC corresponds to the capacitor made with MnO_2 + 5 wt% PANI. Studies were carried out with only three compositions (i.e.; 5, 10 and 20 wt% PANI) of the MnO_2+PANI composite. Among these compositions, specific capacitance of MnO_2+5 wt% PANI is found to be the highest. A narrow variation of composition around 5 wt% PANI may lead to an optimum composition with a marginal increase in specific capacitance, which is not attempted in present study. In the case of electrochemical capacitors, each electrode is generally considered as a capacitor with one charged surface on the solid electrode and the other charged layer in the solution side. Thus a capacitor with two electrodes is considered as a combination of two capacitors in series. If C is the capacitance of each electrode (assuming the same mass of active material on both electrodes), total capacitance (C_T) of the two-electrode capacitor is given by $C_T = C/2$. Therefore, capacitance values of individual electrodes with 0, 5, 10 and 20 wt% PANI are 23.2, 34.4, 29.8 and 12.2 F, respectively, and the corresponding SC values of the two electrodes are 131.2, 204.0, 188.8, and 104.4 F g^{-1} (on the basis of MnO_2 mass). The specific capacitance values for powder MnO_2 samples ranging from 150 to 250 F g^{-1} are reported in the literature [10-15]. The value depends on experimental condition such on current density, potential range, area of the electrode, specific mass of the active material and the nature of the electrolyte. In the present study, the value of specific capacitance (204 F g^{-1}) obtained for MnO_2 + 5 wt% PANI is within the range generally reported. It is worth noting that the electrode area (9 cm^2) and the specific mass are also high (20 mg cm^{-2}). Studies with large area electrodes with high specific mass are considered as important for development of commercial supercapacitors.

Cycle-life test : Capacitors assembled with 0, 5, 10 and 20 wt% PANI were subjected to cycling for 50 charge-discharge cycles with 25, 50, 100 mA and the data are presented in Fig. 4.

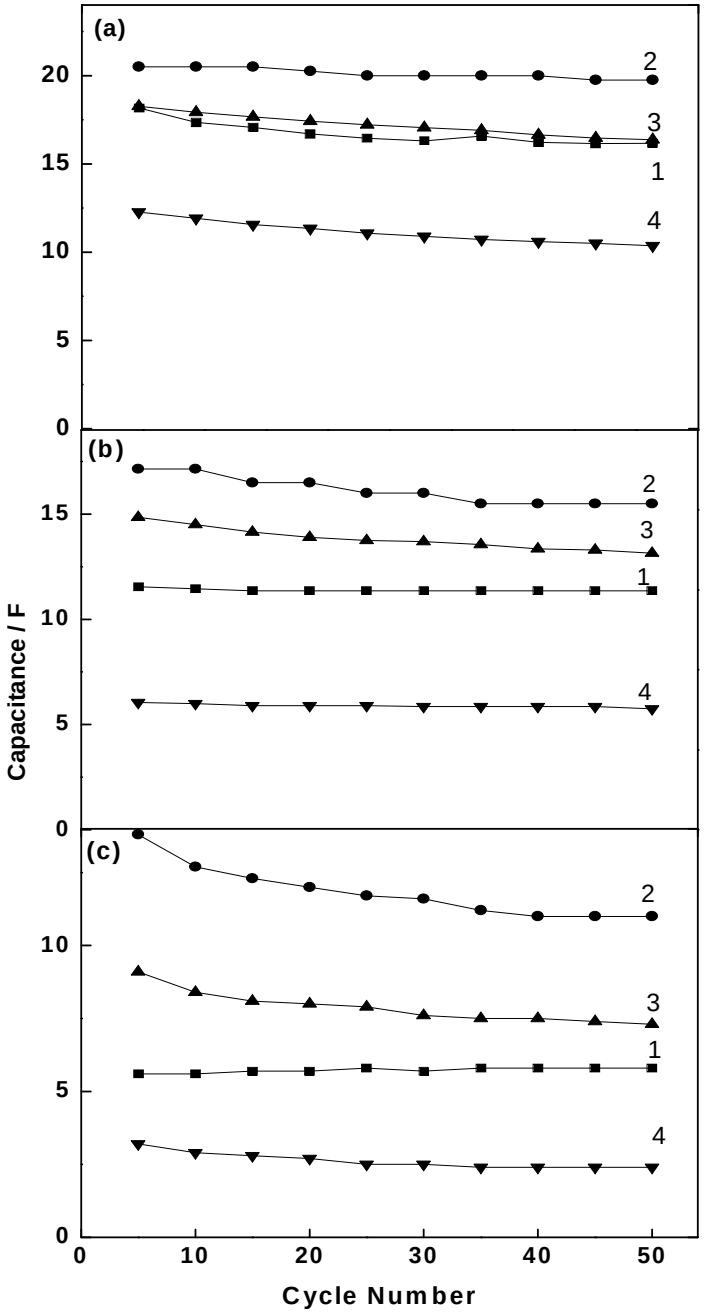

Fig. 4 Capacitance measured for 50 charge-discharge cycles at (a) 25, (b) 50 and (c) 100 mA for MnO_2 capacitors with (1) 0, (2) 5, 10 (3) and 20 wt% (4) PANI.

It is seen that capacitance is fairly stable over 50 charge-discharge cycles for all capacitors, and at all currents tested. However, for all currents, capacitance of MnO_2+5 wt% PANI capacitor is

greater than the rest of the capacitors. The MnO_2 and MnO_2+5 wt% PANI capacitors were subjected to continuous 1000 charge-discharge cycles at 100 mA current. The discharge capacitance data and coulombic efficiency are presented in Fig. 5.

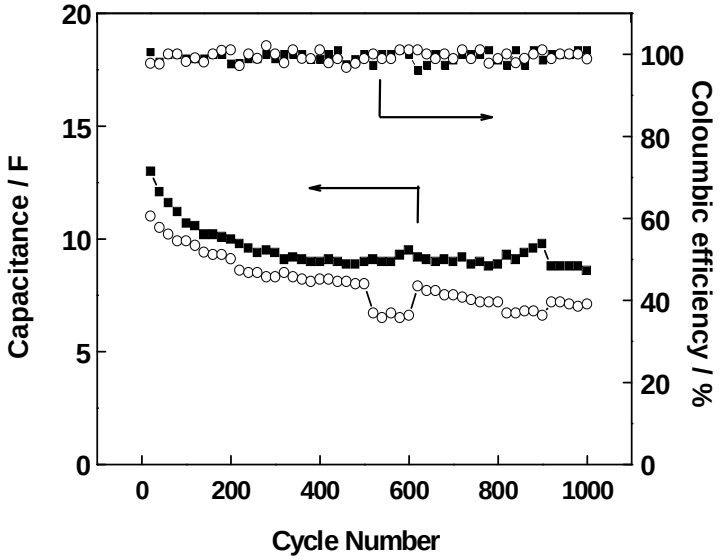

Fig. 5 Discharge capacitance and coulombic efficiency of capacitors made with MnO_2 (o) and MnO_2 + 5 wt % PANI (•) at a charge-discharge current of 100 mA.

The capacitance of MnO_2+5 wt% PANI capacitor is greater than that of MnO_2 capacitor throughout the cycle-life tested. The initial capacitance of the former capacitor is about 13 F and it gradually decreases to a stable value of about 10 F. On the other hand, the initial capacitance of MnO_2 capacitor is 11 F and it decreases gradually to a stable value of 8 F in about 200 cycles. Stable capacitance values are obtained for rest of cycle-life tested. These data suggest that the capacitor made using MnO_2+5 wt% PANI composite is expected to be stable over an extended charge-discharge cycling the capacitance of MnO_2+5 wt% PANI capacitor is higher than that of MnO_2 capacitor. Furthermore, the coulombic efficiency of both capacitors is close to 100 % (Fig. 5). An examination of the cycled electrodes by scanning electron microscopy (Figs. 1b and 1d) suggests that there is no noticeable change in morphology of the electrodes.

Equivalent series resistance : As stated previously, a charge-discharge curve (Fig. 3) exhibits a sudden drop in voltage at the start of both charging and discharging. For the data presented in Fig. 3 the voltage drop values during discharge with 50 mA current are 0.30, 0.22, 0.26, and 0.43 V, respectively, for capacitors with 0, 5, 10 and 20 wt% PANI. It is evident that the voltage drop is low for the capacitor made with MnO_2+5 wt% PANI composite. Fig. 6a shows voltage drop versus wt% of PANI in MnO_2+PANI composite for a few discharge currents.

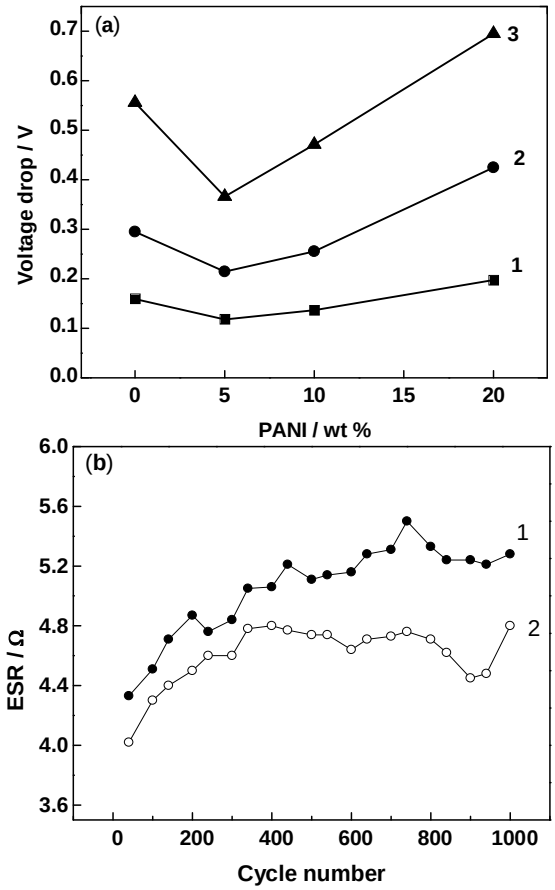

Fig. 6 (a) Voltage drop at the beginning of discharge of capacitors versus percentage of PANI at a current of 25 (1), 50 (2) and 100 mA (3). (b) ESR versus cycle number for MnO_2 (1) and MnO_2+5 wt% (2) PANI capacitors.

At all currents the voltage drop is low for the MnO_2+5 wt% PANI capacitor. At 100 mA discharge current for instance, the voltage drop is 0.55 V for the MnO_2 capacitor, whereas it is only 0.35 V for the MnO_2+5 wt% PANI capacitor. With an increase of PANI content in the composite there is an increase in voltage drop. At low concentration of PANI, the MnO_2 particles are covered with a thin layer of the conducting polymer, which favours an efficient inter-particle contact, thus, reducing internal resistance. At higher concentrations, however, thick layers of PANI increase electronic resistance because of poor conductivity of PANI in neutral electrolytes. Using the value of voltage drop (ΔV) and the current (I), internal resistance ($R_i = \Delta V / I$) of the capacitor was calculated for each value of the current. The R_i can be considered as the equivalent series resistance (ESR) of supercapacitors. The average values of ESR calculated from three currents (25, 50, and 100 mA) are 5.9, 4.2, 6.0 and 7.7 Ω for capacitors made of MnO_2 with 0, 5, 10, and 20 wt% PANI. Thus the capacitor made with MnO_2+5 wt% PANI has the least ESR. Furthermore, the values of ESR of MnO_2 and MnO_2+5 wt% PANI capacitors were calculated during the course of cycle-life test (Fig. 5), and shown in Fig. 6b against cycle number. The ESR of MnO_2+5 wt% PANI is less than that of MnO_2 capacitor throughout the cycle-life test. Thus, a

higher capacitance and also a lower ESR are the advantages gained from 5 wt% PANI in the composite of MnO_2+PANI.

Fig. 7a shows capacitance versus discharge current for MnO_2 and MnO_2+5 wt% PANI capacitors. The capacitance of MnO_2+5 wt% PANI is about 22 F at low currents, but it decrease by increasing current. Capacitance of about 8 F is obtained at 140 mA charge-discharge current. Nevertheless the influence of PANI is clearly evident, as the capacitor of MnO_2+5 wt% PANI has greater capacitance and also lower ESR

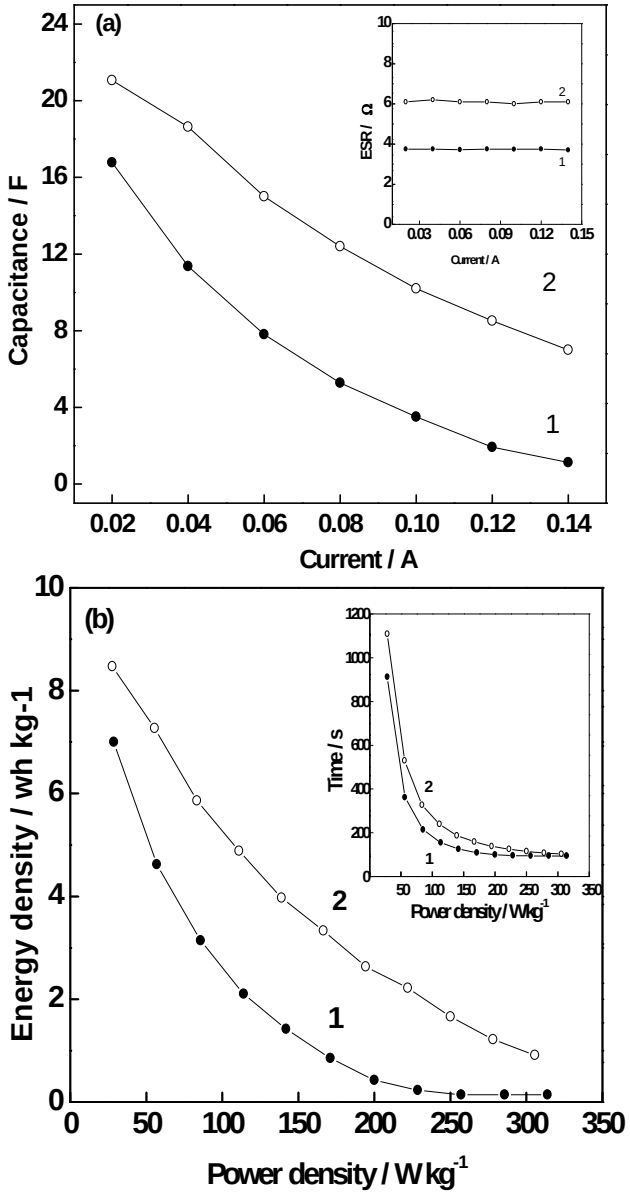

Fig. 7 (a) Capacitance versus current and (b) energy density versus power density for MnO_2 (1) and MnO_2 + 5 wt % PANI (2) capacitors. Plots of ESR versus current and discharge time versus power density are shown as insets of (a) and (b), respectively.

(Fig. 7a inset) at all currents. Energy density (ED) and power density (PD) of the capacitors were calculated using Eqns. (4) and (3).

$$ED = V\ I\ t\ /\ (2\ m) \quad (3)$$

$$PD = V\ I\ /\ (2\ m) \quad (4)$$

Where t is discharge time and m is mass of MnO_2 on both electrodes the capacitor. The mass of MnO_2 alone in the composite was used for calculations. ED versus PD curves for MnO_2 and MnO_2+5 wt% capacitors are shown in Fig. 7b. At low PD as expected, there is a high ED and also high discharge time (Fig. 7b inset). But ED and also discharge time decrease with an increase in PD. The positive effect of PANI present in the composite is clearly reflected in Fig. 7b.

Electrochemical impedance spectroscopy : Electrochemical impedance spectra of capacitors made with MnO_2 and MnO_2+5 wt% PANI were recorded during the course of cycle-life study (Fig. 5). Cycling was stopped after every 100 charge-discharge cycles, the capacitors were rested for 30 min., impedance spectra were recorded at open circuit condition (~ 0.0 V) and thereafter the cycling was resumed. Nyquist and Bode impedance plots recorded after the initial 100 cycles for MnO_2 capacitor are typically presented in Fig. 8. Similar spectra were recorded for MnO_2+5 wt% PANI capacitor and also at all stages of cycle-life test for both capacitors. The Nyquist impedance spectrum (Fig. 8a) consists of high frequency intercept on the real axis, a semicircle and linear low frequency spike. The nature of this figure is different from the Nyquist plots of dielectric capacitors and carbon-carbon symmetric capacitors, which do not consist of any semicircles [31]. In carbon based capacitors, the origin of supercapacitor is due to a accumulation of ionic charges without involving an electron transfer process, whereas the Mn^{4+}/Mn^{3+} redox process (reaction 1) results in accumulation of ionic charges in MnO_2 based supercapacitors. The high frequency intercept in Fig. 8a corresponds to the ohmic resistance (R_s) of the capacitor, which is contributed by electronic resistances of the current collector, leads, electrode material, electrolyte, etc. In the case of carbon based capacitor, R_s is equal to ESR [31]. However, in the present case, ESR should be the sum of R_s and the resistance due to charge-transfer processes (reaction 1). The appearance of the semicircle between 100 kHz to 8.5 Hz is due to parallel combination of charge-transfer resistance (R_{ct}) associated with the redox reaction (reaction 1) and double-layer capacitance (C_{dl}). The impedance (Z_1) of the system in 100 kHz – 8.5 Hz frequency range is therefore given by

$$Z_1 = R_{ct}\,(1-j\,\omega\,R_{ct}^2\,C_{dl})\ /\ (1+\omega^2\,R_{ct}^2\,C_{dl}^2) \quad (5)$$

The $R_{ct}\ C_{dl}$ time constant (τ_1) is obtained from the frequency (f^*) at the maximum of semicircle as

$$\tau_1 = 1/\ (2\ \pi\ f^*\ ) \quad (6)$$

For the data shown in Fig. 8a, the time constant for charging of the double layer is 0.14 ms, which is calculated from the frequency (f* = 1.16 kHz) at the maximum of semicircle. The diameter of the semicircle is equivalent to R_{ct}. The sum of R_s and R_{ct} (Fig. 8a) is about 2 Ω which is considered to be the value of ESR. This value (2 Ω) is lower than the value (4 Ω) obtained from voltage-drop measurements. This difference is likely to be due to different experimental techniques. Immediately after the semicircle; the linear segment appears to extend to an angle of 45°, which is characteristic feature of diffusion process. The diffusion-limited Warburg impedance (Z_2) is given by

$$Z_2 = \sigma\ \omega^{-1/2} - j\ \sigma\ \omega^{-1/2} \quad (7)$$

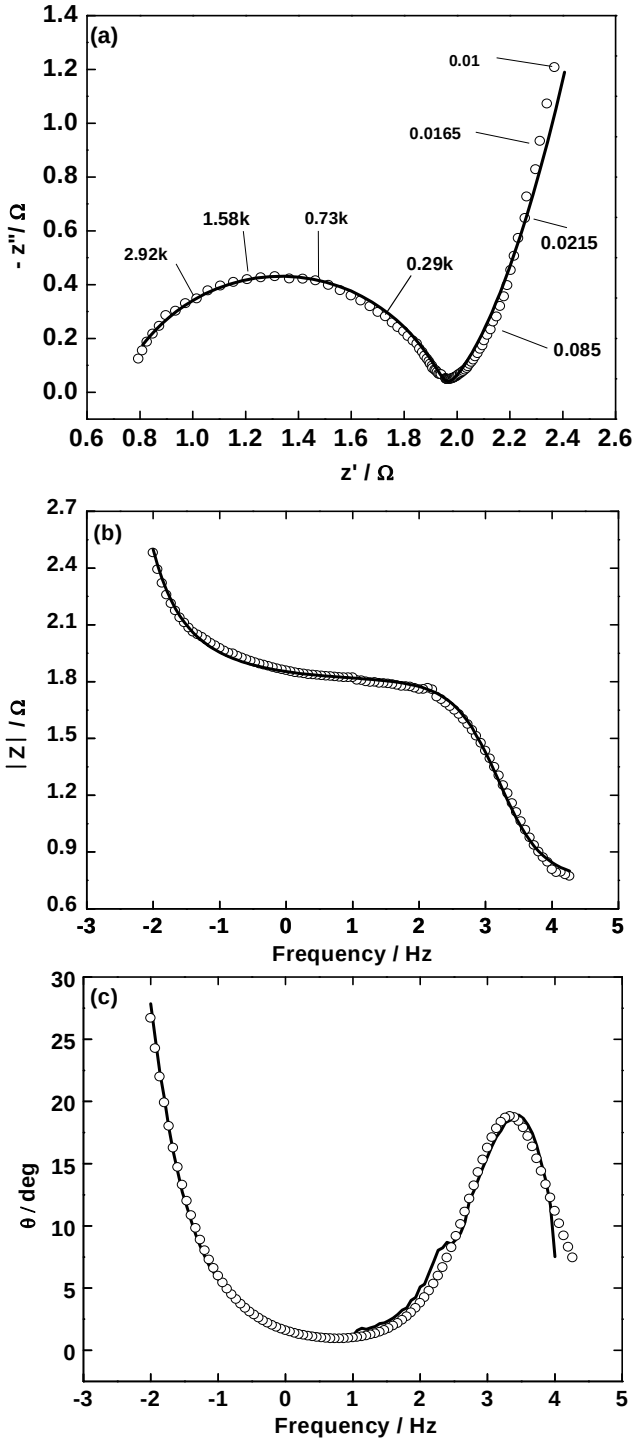

Fig. 8 (a) Nyquist, (b) Bode impedance (|Z|) and (c) Bode phase angle (θ) plots of MnO_2 capacitor after 100 charge-discharge cycles at 100 mA. Experimental data are shown as open circles and the theoretical curves generated from the fit results by a smooth curve.

Where σ is Warburg coefficient, which is related to diffusion coefficient and concentration of the diffusing species. However, this Warburg region exists only in a minor frequency range from 1.0 Hz to 0.25 Hz, which was observed from the linearity of Z" versus $\omega^{-1/2}$ plot (Fig. 9a). In the low frequency region (< 0.25 Hz), the linear spike (Fig. 8a) tends to become parallel to the imaginary axis. A straight line regime parallel to the imaginary axis is the characteristic feature of a capacitor. Thus the low frequency region is attributed to pseudocapaitance (C_φ) of the capacitor. The impedance of system (Z_3) in this frequency region is given as

$$Z_3=1/(j\ \omega\ C_\varphi) \quad (8)$$

The capacitive and resistive regions are also clearly observed in Bode plots (Figs. 8b and 8c). The low frequency pseudocapaitance region is characterized by a decrease in |Z| with log f (Fig. 8b) and also by a decrease in phase angle from - 25° against log f (Fig. 8c). The double-layer capacitance region is reflected by another sloping region (Fig. 8b) between 10 kHz and 85 Hz and also by a - 18° peak in phase angle at 2.1 kHz (Fig. 8c).

On the basis of the various processes of the impedance spectra as explained above, the appropriate electrical equivalent circuit, which was found fit the experimental data is shown in Fig. 9b. Constant phase elements (CPEs) were used in place of capacitances because of inhomogeneous nature of the electrodes. The impedance spectra were subjected to non-linear least squares (NLLS) fitting program, and impedance parameters were obtained. Impedance spectra generated from the fit results and the experimental spectra coincide and χ^2 values are less than $1x10^{-3}$ suggesting the fitting procedure adopted is satisfactory. The impedance parameters of symmetric MnO_2 and MnO_2+5 wt% PANI capacitors recorded during the cycle life study (Fig. 5) were obtained from fit results. It was found that the values of pseudocapacitance (C_φ) were in the range of tens of Farads and the double-layer capacitance (C_{dl}) were in the range of $1x10^{-4}$ F. The variations of C_φ and R_{ct} with cycle number are shown in Fig. 10 for MnO_2 and MnO_2+5 wt% PANI capacitors. It is seen that there is a decrease in C_φ and an increase R_{ct} during initial stages of cycling and the variation is negligibly small thereafter. Furthermore, the R_{ct} is

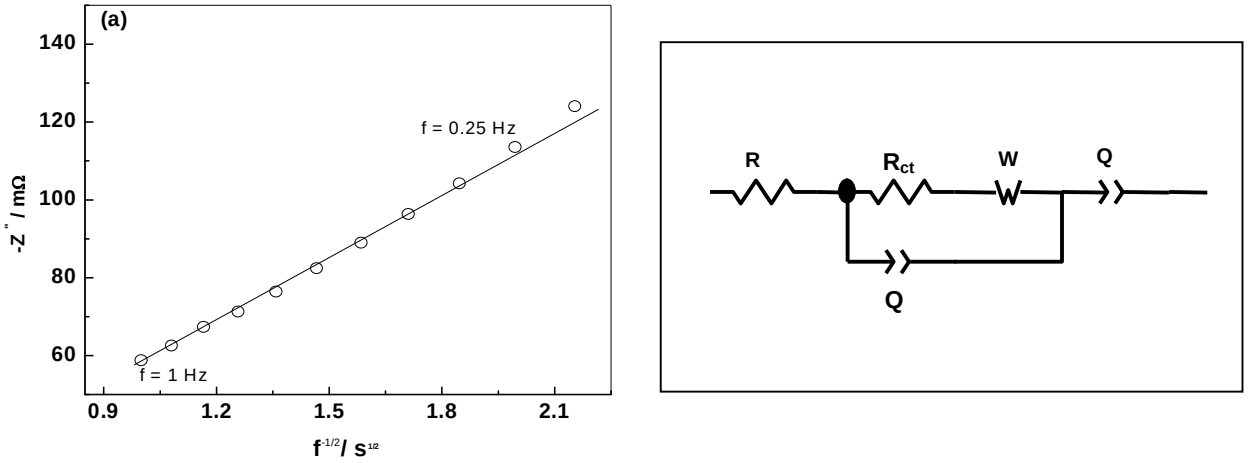

Fig. 9 (a) Variation of Z" with $1/f^{1/2}$ in frequency region from 1.0 Hz to 0.25 Hz, and (b) equivalent circuit employed for curve fitting. Q_1 and Q_2 are CPEs used in place of C_{dl} and C_φ, respectively. See text for the other symbols.

lesser and C_φ is greater for MnO_2+ 5 wt% PANI capacitor than for MnO_2 capacitor. The time constant (τ_2) for the pseudocapacitance is calculated from eq. (9).

$$\tau_2 = (R_s + R_{ct})\ C_\varphi \quad (9)$$

For the data shown in Fig. 8, the time constant calculated is 42 s. Hence, the supercapacitors made with MnO_2 and MnO_2+5 wt% PANI can be subjected to fast charging.

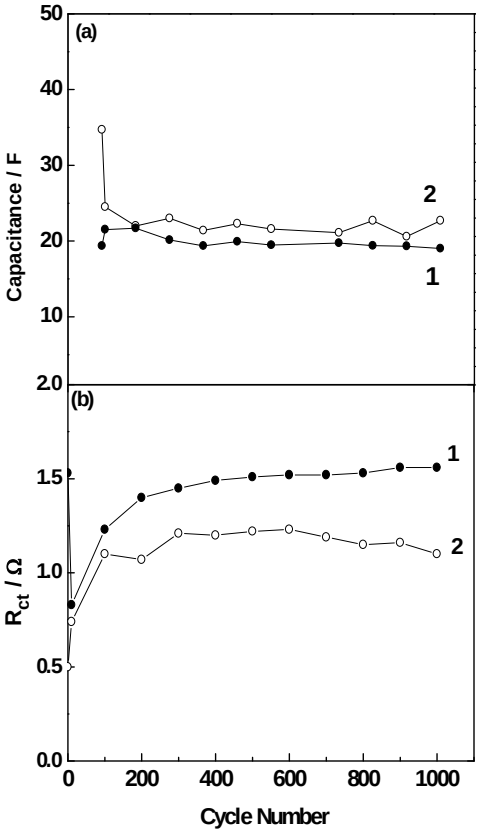

Fig. 10 Variation of (a) pseudocapacitance (C_φ) and (b) charge-transfer resistance (R_{ct}) of MnO_2 (1) and MnO_2 + 5 wt% PANI (2) capacitors with cycle number

APPLICATIONS

MnO_2 + PANI composites studied and supercapacitors fabricated with MnO_2 + 5 wt% PANI provides a high capacity and a low equivalent series resistance. These can be suitable in making commercial capacitors.

CONCLUSION

Large area electrodes of MnO_2+PANI composites of several compositions are fabricated with high specific mass of the active materials and laboratory scale prototype symmetric capacitors are assembled. The results of long-cycle life test conducted for the capacitors suggest that the capacitance of MnO_2+5 wt% PANI capacitor is greater than that of MnO_2 capacitor. Furthermore, the equivalent series resistance of the former capacitor is less than the later capacitor. Ac impedance measurements suggest that the charge-transfer resistance gradually increases during the initial stages of cycling and thereafter remains nearly stable. From all these experimental studies, it is evidence that the addition of PANI to MnO_2 produces beneficial results.

REFERENCES

[1] B. E. Conway, "Electrochemical Supercapacitor: Scientific Fundamental and Technological Application", Plenum Publisher, New York, (**1990**) p.1
[2] S. Sarangapani, B. V. Tilak and C. P. Chen, J. Electrochem. Soc. 143, 3791 (**1996**)
[3] M. M. Thackeray, Prog. Solid State Chem. 25, 1 (**1997**)
[4] O. Bricker, Am. Mineral. 50, 1296 (**1965**)
[5] A. J. Salkind, J.J. Kelly and A. G. Cennone in D. Linden (Ed.), "Handbook of Batteries", McGraw Hill, New York (**1995**) p.1
[6] S. U. Falk and A. J. Salkind, "Alkaline Storage Batteries", Wiley, New York (**1969**) p.1
[7] S. Devaraj and N. Munichandraiah J. Phys. Chem. C 112, 4406 (**2008**)
[8] O. Ghodbane, J. L. Pascal and F. Favier, Appl. Mater. Inter. 1, 1130 (**2009**)
[9] H. Y. Lee and J. B. Goodenough, J. Solid State Chem. 144, 220 (**1999**)
[10] T. Brousse, Z. M. Toupin, R. Dugas L. Athouël, O. Crosnier and D. Belanger, J. Electrochem. Soc. 153**,** A 2171 (**2006**)
[11] J. K. Chang and W. T Tsai**,** J. Electrochem. Soc. 150**,** A1333 (**2003**)
[12] X. Wang, X. Wang, W. Huang, P.J. Sebastian and S. Gambo, J. Power Sources 140, 211 (**2005**)
[13] Y. U. Jeong and A. Manthiram, J. Electrochem. Soc. 149, A1419 (**2002**)
[14] V. Subramanian, H. Zhu and B. Wei, Chem. Phys. Lett. 453, 242 (**2008**)
[15] P. Ragupathy, D. H. Park, G. Campet, H. N. Vasan, S. J. Hwang, J. H. Choy and N. Munichandraiah, J. Phys. Chem. C, 113, 6303 (**2009**)
[16] D. Belanger, T. Brousse and J. W. Long, Interface 17, 49 (**2008**)
[17] S. Devaraj and N. Munichandraiah, Electrochem. Solid-State Lett. 8, A373 (**2005**)
[18] Z. Zhou, N. Cai and Y. Zhou, Mater. Chem. Phy. 94, 371 (**2005**)
[19] X. Zhang, L. Ji, S. Zhang and W. Yang, J. Power Source 173, 1017 (**2007**)
[20] L. J. Sun and X. X. Liu, Eu. Poly. J. 44, 219 (**2008**)
[21] C. Yuan, L. Sun, B. Gao and X. Zhang, Electrochim. Acta 53, 7039 (**2008**)
[22] W. Zou, W. Wang, B. He, M. Sun and Y. S. Yin, J. Power Source 195, 7489 (**2010**)
[23] W. Ni, D. Wang, Z. Huang, J. Zhao and G. Cui, Mater. Chem. Phys. 124, 1151 (**2010**)
[24] W. Zou, W. Wang, B. He, M. Sun and Y. Yin, J. Power Source 195, 7489 (**2010**)
[25] Q. Li, J. Liu, J. Zou, A. Chunder, Y. Chen and L. Zhai, J. Power Source 196, 565 (**2011**)
[26] P. Ragupathy, H. N. Vasan and N Munichandraiah, J. Electrochem. Soc. 155, A34 (**2008**)
[27] D. C. Trivedi, in H.S. Nalwa (Ed.), "Handbook of Organic Conductive Molecules and Polymers", Vol. 2, Wiley, New York (**1997**) p. 504
[28] S. K. Mondal and N. Munichandraiah, Electrochim. Acta 52, 3258 (**2009**)
[29] C. Xu, H. Du, B. Li, F. Kang and Y. Zeng**,** J. Electrochem. Soc. 156, A73 (**2009**)
[30] C. Xu, H. Du, B. Li, F. Kang and Y. Zeng**,** J. Electrochem. Soc. 156, A435 (**2009**)
[31] P. L. Taberna, P. Simon and J. F. Fauvarque, J. Electrochem. Soc. 150, A292 (**2003**)